



Automatic post-processing for tolerance inspection of digitized parts made by injection moulding

Michele Bici, Francesca Campana & Alessio Trifirò

To cite this article: Michele Bici, Francesca Campana & Alessio Trifirò (2016) Automatic post-processing for tolerance inspection of digitized parts made by injection moulding, Computer-Aided Design and Applications, 13:6, 835-844, DOI: [10.1080/16864360.2016.1168231](https://doi.org/10.1080/16864360.2016.1168231)

To link to this article: <https://doi.org/10.1080/16864360.2016.1168231>



Published online: 18 Apr 2016.



Submit your article to this journal [↗](#)



Article views: 138



View Crossmark data [↗](#)



Citing articles: 1 View citing articles [↗](#)

Automatic post-processing for tolerance inspection of digitized parts made by injection moulding

Michele Bici^a , Francesca Campana^a  and Alessio Trifiro^b

^aUniversità di Roma "La Sapienza", Italy; ^bABB SpA, Pomezia, Italy

ABSTRACT

This paper presents the advancements of an automatic segmentation procedure based on the concept of Hierarchical Space Partitioning. It is aimed at tolerance inspection of electromechanical parts produced by injection moulding and acquired by laser scanning. After a general overview of the procedure, its application for recognising cylindrical surfaces is presented and discussed through a specific industrial test case.

KEYWORDS

Computer aided tolerancing & inspection; Injection moulding; Reverse engineering; Hierarchical space partitioning

1. Introduction

Injection moulding is one of the most widespread manufacturing systems for high volume production. In case of electromechanical components (dimensional range between 25–150 mm, shell thickness 0.5 mm), Reverse Engineering (RE) may play an important role to understand weakness of the product-process design. Arrangement of the cavities on the die may locally change injection and cooling parameters, producing sinks, weld lines, burrs or global shape defects (warpage). Residual stresses induced by shrinkage are major responsible of these defects and, of course, they affect dimensional and geometrical tolerances of the parts. For this reason, in electromechanical assemblies, inspection of functional tolerance represents a relevant aspect to validate die design, in particular if a large amount of parts is made as multiple cavities on a single die [3], [6]. Although the injection moulding process has a tolerance compatible with laser scanner measurements (± 0.05 mm versus an accuracy of 0.025 mm) or other enhanced solutions (e.g. grey code and phase shift systems), RE applications concerning the evaluation of dimensional and geometrical tolerances are not a well-established industrial tool yet. It is due to methodological problems associated to: (1) the post-processing of the cloud of points, (2) the assessment of the measurement protocol; (3) the hardware set-up according to the acquisition paths and conditions [10],[13]. As a consequence of these problems suitable software, able to aid the RE inspection through automatic analysis of the components, is still missing.

In [7] an exhaustive state of the art concerning RE for tolerance inspection is presented together with a general frame for evaluating Geometrical Product Specification according to ISO standard. Nevertheless the attention is mainly focused on how extract the tolerance value not on the post-processing automation. In [4] we analyse the inspection process usually made by a Co-ordinate Measurement Machine and that one based on RE techniques. RE techniques may support the automation of the inspection process mainly through a segmentation based on part type recognition. Doing so the component shape can be rebuilt and analysed without asking for CAD alignment. It is particularly interesting to avoid user interaction, when a large amount of inspections are required, as in the case of the injection mould set-up. The preliminary set-up of this automation has been discussed in [4] and applied to recognize planar surfaces of a din rail clip made by injection moulding. In [5] the din rail clip and an axial-symmetric aeronautical flange have been investigated to evaluate the feasibility of cylindrical surfaces recognition and the computation of a component reference system, named Intrinsic Reference System (IRS). It has been made with the aim of align the cloud of points in the space, without the necessity of knowing the CAD alignment or adopting the reference system of the acquisitions.

In this paper, we continue this endeavour discussing the enhancements made to enlarge the capability of the method, in particular: (1) the algorithms we adopted for finding and clustering cylindrical surfaces; (2) some

improvements on the evaluation of the thresholds necessary to partition the surfaces and (3) the computation of the IRS.

In Section 2, a brief summary of the proposed post-processing is given to allow the comprehension of the enhancements described in Section 3, then in Section 4 by means of a test case their effectiveness is shown and finally in Section 6, after a general discussion made in Section 5, the main conclusions are outlined.

2. Segmentation procedure through hierarchical space partitioning

Feature segmentation represents one of the most relevant aspects for developing automatic inspection of digitized shapes. Ordinarily, in the RE of mechanical components gradient analysis is one of the most adopted solution [2], [11], especially in case of free-form shapes. It is generally applied on the tessellated surface or on a suitable reduction obtained replacing each triangle with its centroid. Therefore, it is clear that the accuracy of the analysis is extremely tied to the number of points, their density and distribution. To reduce computational time, point cloud filtering is one of the most adopted solutions but in case of tolerance inspection it can lead to a loss of results, especially if the evaluation of the global shape distortion is also required. Electromechanical components manufactured via injection moulding are characterized by planar and cylindrical surfaces with sharp angles, low thicknesses and many small ribs. In these cases surface reconstruction of a filtered acquisition may not represent a good solution if it must be used for tolerance inspection on a large number of samples. Adopting a segmentation algorithm based on a voxel approximation of the component, we can analyse the surface recognition problem according to a scale larger than the tessellated mesh, without applying preliminary filters.

The voxel approximation is derived from the concept of Hierarchical Space Partitioning [9]. A virtual 3D structure is superimposed to the cloud of points, like a bounding box, and then, this structure is subdivided into elementary volumes (becoming the voxel structure) in which the presence of points makes a voxel treated as in a binary system. Its value is “1” (true state) if it includes points of the cloud, “0” (false state) if it does not. The creation of the structure starts from a single voxel and then, along each direction, it is recursively split into smaller voxels (every voxel is subdivided into 8 smaller voxels at each iteration) until no more points are included or an imposed maximum number of subdivisions is reached. The maximum number of subdivisions determines the

voxel length along the i^{th} direction, according to the equation:

$$Length_i = \frac{\max(P_i) - \min(P_i)}{2^{r_i}} \quad (1)$$

where $i = x, y, z$ and r_i is assumed to be the algorithm’s resolution. It changes at each iteration, until the maximum number of subdivisions (2^{r_i}) is reached along each direction. At the end of the computation, false state voxels are not considered so that the plot of true state voxels is able to represent a rough estimation of the component shape. Fig. 1 gives two examples of the “true state” voxels surrounding the cloud of points. On the left the resolution is set to 8 voxel in each direction, on the right to 32. In [4] the sensitivity to the algorithm’s resolution is discussed, highlighting that a satisfactory voxel’s length must be chosen: (a) to limit the inclusion in one voxel of different features (like planes with chamfer, radii, edge, . . .); (b) to assume a proper resolution able to aggregate together voxels with similar local surface characteristics; (c) to build the whole surfaces that must be inspected.

If a voxel includes a sufficient number of points, that are representative of a local small area of a feature, best-fit algorithms can evaluate the local characteristics of basic surfaces. As already said, since in electromechanical components made by injection moulding planar and cylindrical surfaces are the most frequent kind of features, the proposed post processing evaluates the local feature inside the true state voxels through a planar surface algorithm. If the local surface is found to be planar it is ready for plane segmentation, and its voxel is named “planar voxel”, otherwise it is named “curved voxel” and analysed to evaluate if it can be fit by a local cylindrical surface.

In [4], the criterion to evaluate if the points inside a voxel represent a local planar surface has been based on a threshold derived from the statistical distribution of the variance of the point distances from the voxel’s best-fit planes. Although this assumption is affected by the acquisition accuracy, in [4] and [5] the effectiveness of this criterion to distinguish local planar surfaces from the other types was discussed through real test cases. In Section 3 and 4, an enhancement of this criterion is presented and tested to improve the accuracy for partitioning planar and curved surfaces.

The plane segmentation aims to set planar voxels according to the peculiar directions of the component. It groups together voxels with similar directions and finds planar faces (named also clusters). It is made through an hybrid region growing – hierarchical clustering procedure that sets together the planar voxels according to a

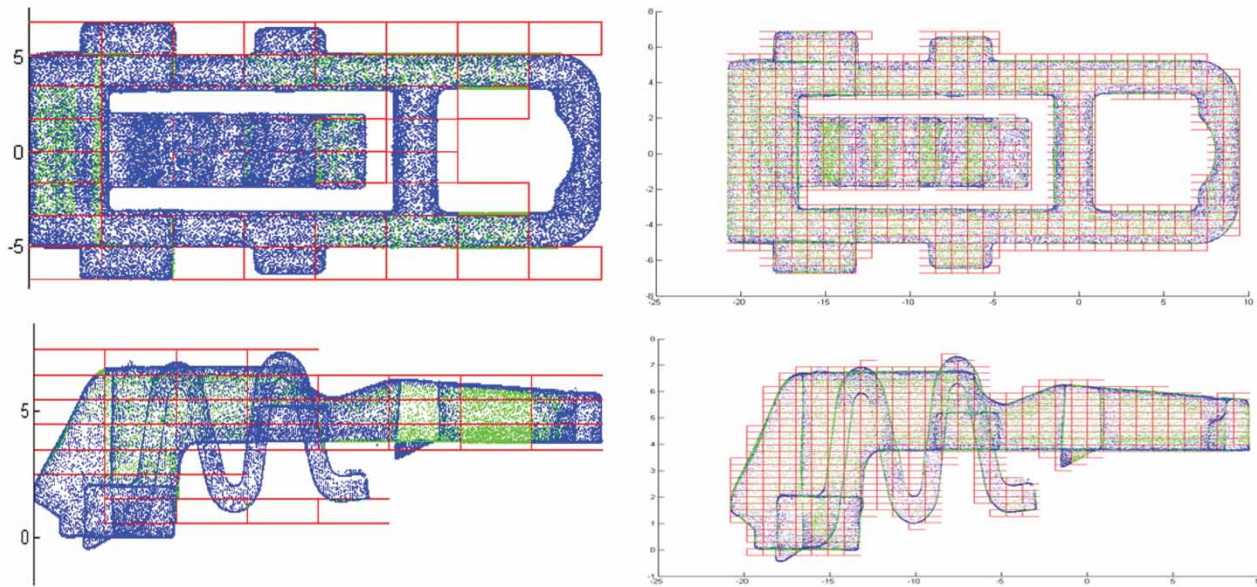


Figure 1. Voxel structure made through true-state voxels. On the left $8 \times 8 \times 8$; on the right $32 \times 32 \times 32$.

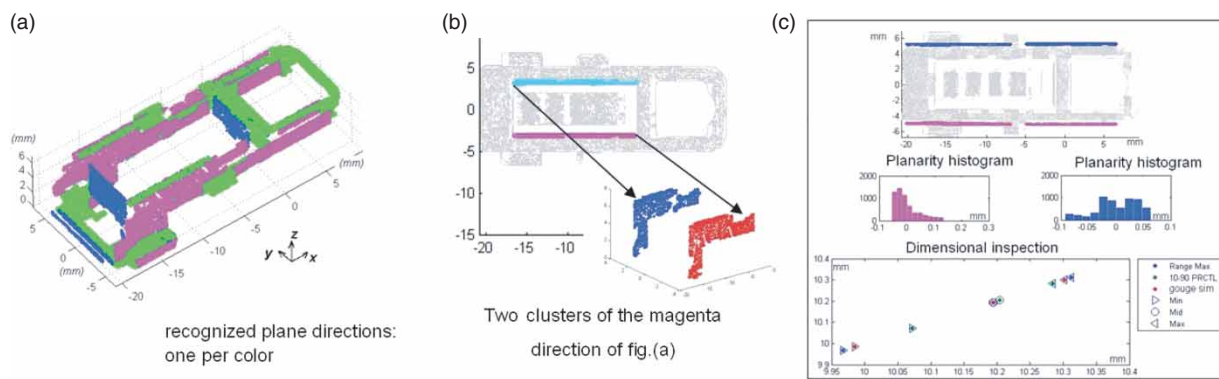


Figure 2. (a) Region growing of the elementary planes, (b) example of two distinct planar surface (clusters) of the set, (c) example of tolerance inspection diagrams between two distinct planar clusters.

threshold condition derived from the so-called L2 orientation norm as discussed in [11]. If a generic planar voxel does not belong to any set, it is adopted as new seed of a new direction. Obviously the first seed is the first planar voxel to be analysed. Doing so the segmentation algorithm is able to recognize peculiar directions of the components automatically [4]. Successively, a hierarchical clustering process is able to check connections of proximity among planar voxels that are included in the same direction set. If the check is positive the cluster that represents a component face is enlarged.

Fig. 2 gives an example of the results achieved by the proposed approach according to one of the test case already presented in [4] and [5]. Fig. 2(a). shows the results of the segmentation of the planar directions

(3 normal directions, one per color). Fig. 2(b). and Fig. 2(c). show two examples of parallel faces (clusters) taken from the magenta direction of Fig. 2(a).

Fig. 3 summarizes the proposed approach (on the left) and the applied methodologies (on the right) including also the recent new developments, that are the cylinder partition and the IRS definition (in figure named as “Intrinsic Ref. System”). From this workflow the implementation scheme of the procedure can be described. It is being developed in MatlabR2012. The “Voxel structure” step has been implemented using the parallel computation, region growing and hierarchical clustering have been approached via sparse matrices. Since the logical approach for Plane and Cylinder partition is based on the same methodology the adoption of distributed

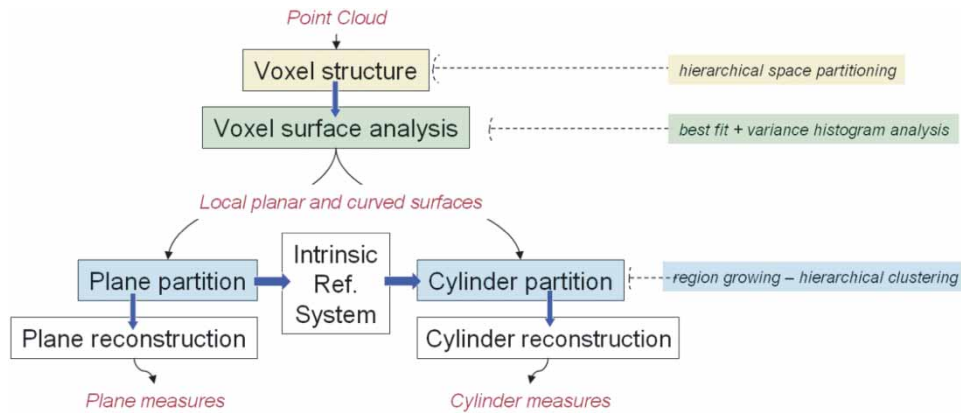


Figure 3. Logical workflow of the proposed approach and applied methodologies (on the right).

computation is investigated to perform hierarchical clustering of planes and cylinders at the same time, after the region growing of the planar voxels.

3. Recent new developments

3.1. Intrinsic reference system of the component

The segmentation procedure recognizes the planar faces of the components notwithstanding the orientation of the point cloud during the acquisition. It can be misaligned with effective principal directions of the component or with the axes system of the CAD model. From the tolerance measurement point of view, an appropriate alignment could be necessary to localize datum or specific sets of functional planes according to draft annotations. It becomes of utmost interest in case of automatic inspection.

Although in [4] we proposed to find the specific features of the component via image analysis of the voxel structure, the industrial version of the proposed procedure left this kind of elaboration and set an automatic recognition of the couple of planes to be measured, through the adoption of an Intrinsic Reference System (IRS). The IRS is found looking for the plane directions associated to the most populated sets of voxels. In case of electromechanical components it may be considered a consistent reasoning since they are characterized by functional features on orthogonal planes or cylinders whose axes are parallel to the three principal directions of the component. Thus it is clear that the most populated sets of voxels are the ones, which contain planar surfaces oriented along component's principal directions. The IRS computation derives by assigning as first reference axis the planar direction of the most populated set of voxels. Then the other two axes are found among the two subsequent more populated sets of voxels that are mutually orthogonal. The soundness of this procedure has

been tested on different components as reported in [5]. The IRS has been always found and it is always associated to the most relevant surfaces of the component (e.g. in case of the axial-symmetric part of Fig. 5(a). it has the z-axis coincident with the central axis of the component). Nevertheless when the entire inspection process will be definitively set up more accurate investigations will be planned to evaluate its consistency with the inspection procedure.

3.2. Local cylindrical surface recognition

As described in section 2 the segmentation process divides voxels in two sets: planar and curved voxels. The first ones have planar features inside and the others non-planar features. Generally speaking, inside the curved voxels can be present not only cylindrical features (cylinders, rounds, . . .) but also edges surfaces with chamfers and points on different planes. To recognize cylinders again we adopt the concept of best-fit and its evaluation through the variance of the distances of the voxel's points compared to the best-fit parameters. To simplify the fitting problem, we work projecting the points inside every curved voxel on planes that are normal to the directions of the IRS' axes and located at the centroid of the points. This is consistent with the assumption that cylindrical features are oriented along principal directions of the components (the IRS) due to their function of latch or hinge. Moreover, it reduces the complexity of the fitting problem, allowing the dealing with algorithms such as Taubin, Kasa or Levenberg-Marquardt (LM) [8], [12].

Circle best-fit can be approached by geometric or algebraic fits. In the first case the unknown parameters (position of the center, C and radius, R) are found through an iterative regression process while in the second case by a system of linear equations. Taubin and Kasa are algebraic approaches instead LM is a typical regression method. Kasa is the fastest method that

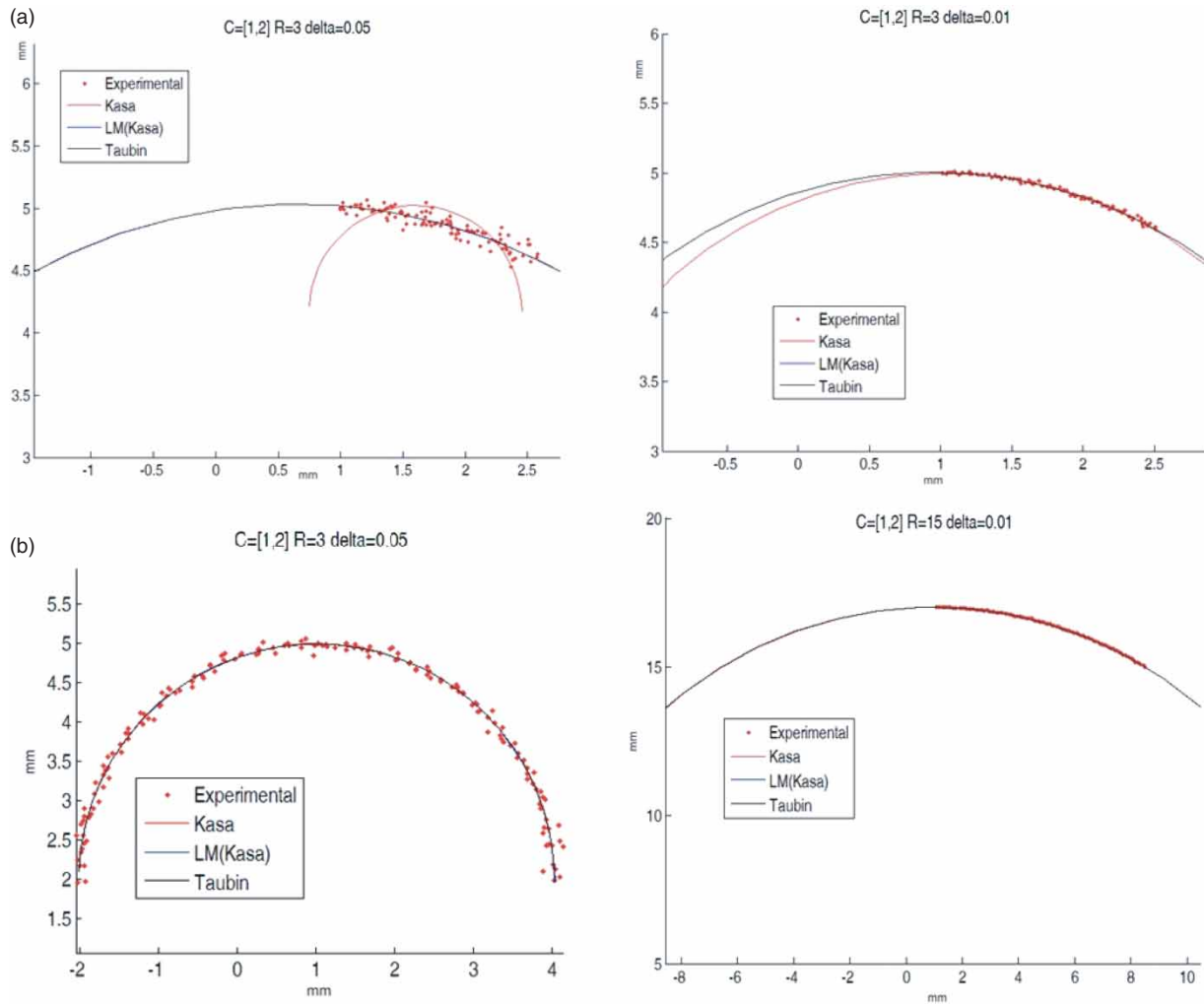


Figure 4. Comparison between circle fit algorithms, (a) noise effect (δ) on small radius; (b) arc length size effect on small and large radius.

works with good results in case of complete circles but it loses accuracy in case of points along arcs with small diameters [1]. Regression approaches like LM are strictly related to the first guess adoption, moreover local minimum cannot be excluded. To gain a good compromise between accuracy and computation time we decided to couple together Kasa algorithm and LM, referring to it as “LM(Kasa)”. The first one gives a rough estimation of the curved voxel surface, that is used as first guess of the second algorithm. Fig. 4 shows a comparison among Kasa, Taubin and LM(Kasa). More in details Fig. 4(a). shows the effects of changing the maximum range of scattering for the points (± 0.05 and ± 0.01) considering a small radius ($R = 3$ mm) on a small arc length. Kasa confirms its limits, while LM(Kasa) is comparable with Taubin. Fig. 4(b). examines two other conditions. On the left it can be observed a confirmation of the effect of the arc length on Kasa algorithm, while on the right the effect of the adoption of greater radius. In both of these two

cases LM(Kasa) is confirmed as a good competitor of Taubin algorithm.

In Fig. 5 a preliminary result of the adopted algorithm is shown according to the test case given in [5]. As it is clear in Fig. 5(c). the nominal value of R6 is computed in terms of fitting radius as [5.97, 5.98] mm.

3.3. Iterative evaluation of the variance threshold and cylindrical surface clusterization

LM(Kasa) is then applied to all curved voxels projecting their points on IRS planes. Also in this case the presence of a local cylindrical surface inside a voxel must be confirmed, looking for the smallest variance among the three values computed by the projections along the IRS axes. Threshold definition for the cylindrical voxel recognition has major difficulties than planar variance analysis, mainly due to more scattered values, so an iterative algorithm has been set to avoid arbitrary input selection

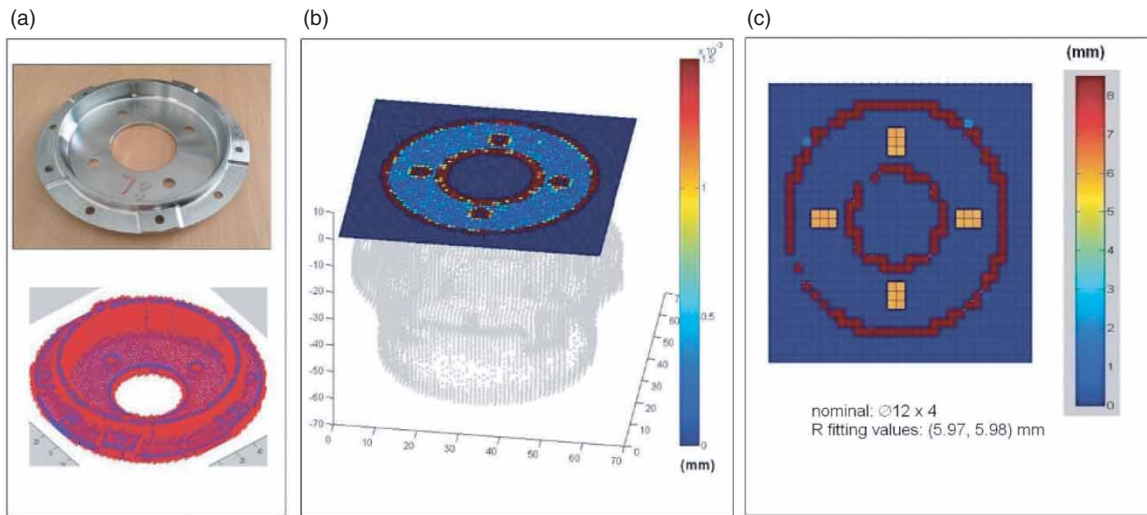


Figure 5. (a) axial-symmetric part acquired to test cylinder recognition and related voxel structure ($64 \times 64 \times 64$), (b) distribution on a voxel section of the planar fitting variance to distinguish curved voxel; (c) Radius fitting values computed on curved voxels.

of the threshold. The variance frequency histogram is now updated splitting its bins until the number of voxels, which are related to the minimum variance, becomes stable. It must be remarked that this iterative algorithm is now applied for finding all the thresholds necessary for the variance histogram analysis. Thus this minimum variance is assumed to be the threshold required for finding the specific type of surface that is under investigation (planar or cylindrical).

Through the same hierarchical clustering procedure applied to planar voxels, cylindrical voxels are then clustered. The selection of the axis directions of the cylinders is automatically done thanks to the projection made to calculate LM(Kasa). As a consequence the region-growing and hierarchical clustering phase is recursively applied for each direction of the IRS. Similarly to the planar surface analysis, it verifies the radius of the cylindrical elementary surface (R_i) to a specific radius (R_j) that represents the current seed of possible cylinder clusterization:

$$DR_{ij} = 1 - \frac{\text{abs}(R_i - R_j)}{R_j} < \varepsilon \quad \forall R_j \in S \quad (2)$$

where ε stands for the threshold assigned to accept R_i as member of the cluster whose R_j is the seed. If eq. (2) is not verified for all the j th elements inside the set of seeds (S), R_i becomes a new member of S . Doing so at the end of the region growing – hierarchical clustering procedure, cylinder clustering is done according to every significant radius R_j of the acquired component that are found in S .

4. Case study

The application analyses a case study able to highlight particularities and problems related to the recent

development of the algorithm. It is a latching lever, utilized in assemblies of electromechanical switches of electric panels (Fig. 6.). The part is made of polyphenylene sulfide (PPS), through an industrial process of plastic injection moulding. Due to its installation and use, the compliance of the nominal values of prescribed dimensions and tolerances is fundamental, mostly in the areas of cylindrical pins, which allow the final housing and functioning in the assembly. The cloud of points has been obtained through a laser scanner (Nikon LC15Dx) mounted on a CMM portal 3 COORD Hera 12.9.7, which allows an accuracy of $2,5 \mu\text{m}$. For the selected sample, after the reconstruction of the complete cloud by the union of the various views, a cloud composed of 62.943 points has been obtained (Fig. 6).

To evaluate the usefulness of the algorithm to cluster planar and cylindrical surfaces, we select a equally spaced voxel structure made of $32 \times 32 \times 32$ cells (32768 voxels), as shown in Fig. 6 on the right. In this figure the cloud of points is represented together with the superimposition of the “true-state” of the voxel structure. They are 3214 compared to the total of 32768 voxels. They include both planar and curved voxels. Among the 3214 voxels we find that 137 have less than 3 points, so that the final number of voxels considered in the analysis are 3077.

In every true-state voxel a local plane is then calculated by best-fit. The variance of the points’ distances from the local planes is used to evaluate if the local set of points can be assumed to be on a planar surface or not. According to sub-section 3.3 it is made also in this case by the research of the threshold applied on the histogram of variances collected from each voxel. The threshold includes as planar voxels only those with variance equal to the bin with smallest variance, after it has been iteratively split until

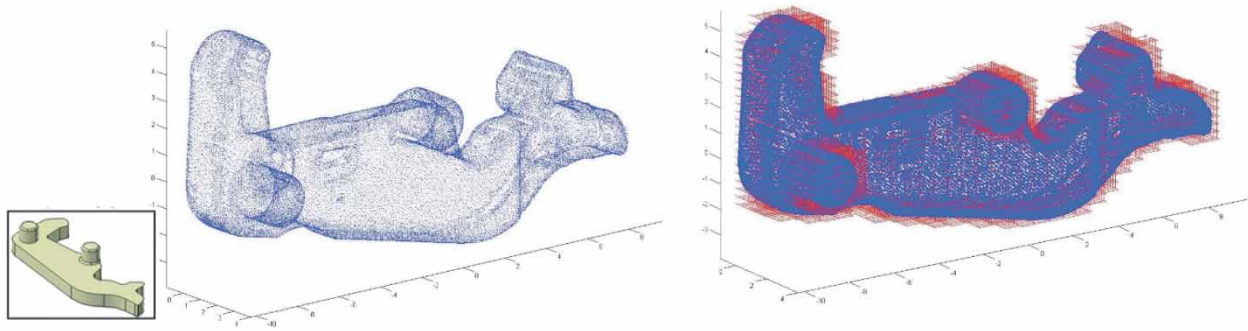


Figure 6. Latching lever: model (in the central box), acquisition (on the left), and $32 \times 32 \times 32$ voxel structure (on the right).

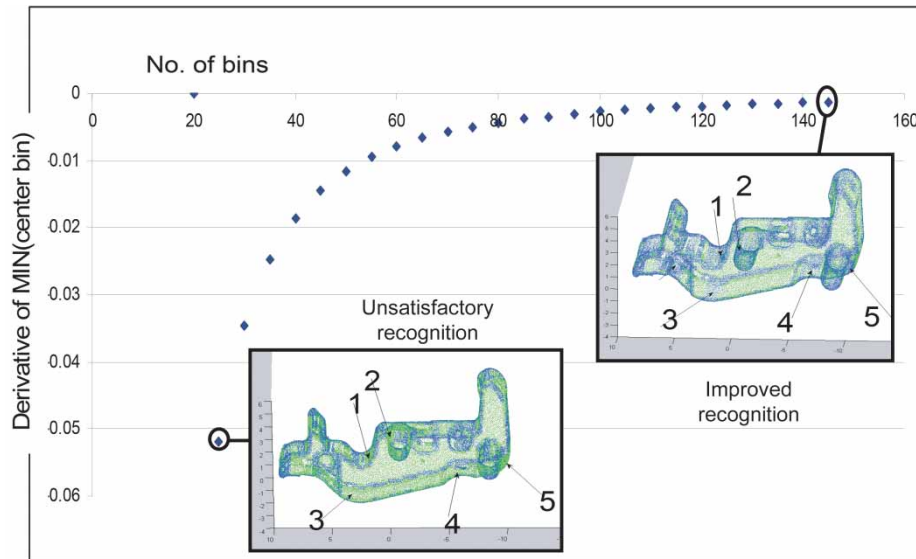


Figure 7. Iterative evaluation of variance threshold for planar voxels (on the left); planar features in green, curved features in blue (on the right).

convergence is reached. Usually, and in particular in this case, we choose to divide the range of the variance histogram starting from an initial value of 20 bins. Fig. 7. shows the results of this iterative research for the case study. The stable value, found increasing the number of bins, can be clearly seen. The component snapshots highlighted in the boxes show the improvements since the new threshold, found at 145 bins, is able to exclude cylindrical areas that locally can be approximated by a plane if the iterative algorithm is not applied (see blue points in areas 1,2,3,4 and 5).

Doing so 1689 planar voxels are found from the 3077 previously defined as “true-state” voxels.

Local planar voxels are then clustered to recognize the component’s planar faces via the hierarchical clustering and region-growing algorithm. Through a L2 norm threshold [4], the local planar voxels are divided in sets in which planes are recognized as parallel. In the considered case, the L2 norm threshold admits an error of 1% between planes’ coefficients.

At this point we have found the sets of parallel planes, and we must consider connections between voxels, to cluster together component’s faces. The results are consistent with the shape of the component that shows large planar faces only normal to the pin axes. Moreover also other small detailed faces are recognized, thanks to the adopted voxel resolution, that allows to find the three principal directions of the component, thus the IRS, as shown in Fig. 8. As already mentioned, in the pieces usually scanned, the cylindrical features appear to have axis directed according to one of these three directions. This remains true in the considered lever, since IRS x-axis is the direction of many cylinders present in the component.

From the segmentation point of view the cylindrical analysis is performed on the remaining curved voxels (1388 voxels), that are highlighted in Fig. 9. It shows that curved voxels contain both vertex surfaces, with or without radii, and not only local cylindrical surfaces.

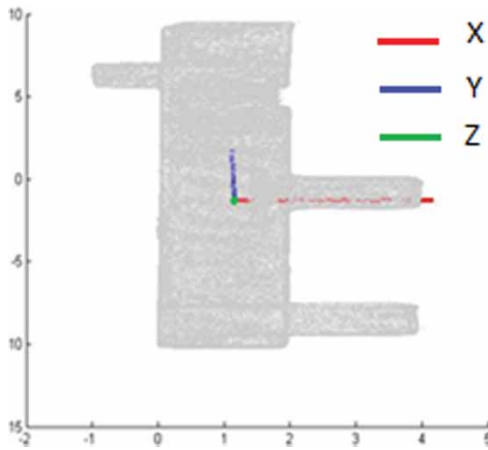


Figure 8. Lateral view of the latching lever with its IRS, applied in the component centroid.

At this point, for each curved voxel three best-fit circumferences are calculated (one for every principal direction), using LM(Kasa), in which Kasa is used to be the first guess of LM. The circumferences are local approximation of the points in the curved voxels, after their projection on the IRS.

Then, only one of the three circumferences for each voxel is selected. It is the one having the minimum value of variance. Analogously to the planar case, we must impose a threshold on the values of variance, to distinguish truly cylindrical voxels from the others.

The algorithm for the automatic selection of the threshold, as previously described, is now applied again for the cylindrical case, three times, once for each principal direction. We start from the same values of first guess of the planar case (20 bins). Results are shown in Tab. 1. The first column reports the values of the first guess of the algorithm for the automatic threshold, the second column reports the optimal number of bins obtained, in

the third column there are the values of the calculated threshold, in the fourth the recognized curved voxels without the iterative computation and in the latest the number of the recognized cylindrical voxels with the iterative computation.

Since in the proposed case study the most voxels with cylindrical feature inside are included in the set with the axes parallel to the X direction, from now on, we consider only this direction.

As we described in Section 3, region growing and hierarchical clustering algorithms are adapted also for the cylindrical case. The voxels are grouped by the values of radius, using the formula (2) in Section 3. In the considered case, we admit a lower threshold than the previous one that has been adopted in case of planar surface clustering, so that, we admit an error of 20% approximately.

The difference between the errors, in the planar case and in the cylindrical one, is mainly due to the two different algorithms of best-fit and clusterization; in the planar case we must set a stricter threshold to avoid the possibility of joining, in the same cluster, local planes that aren't really parallel.

The cylindrical analysis starts from the three principal direction (the IRS of the component), so it requires a less stringent threshold to achieve a good clusterization without loss of data. To validate this assumption a sensitivity analysis must be done as already made in case of planar clusterization [4]. For the X direction, we have the situation reported in Fig. 10(a). It shows, in terms of points, each set of clustered cylinders, one per color. For example green points of Fig. 10(a). are part of the R1 cylinder set of clusters, isolated in Fig. 10(b).

After the cluster recognition cylinder reconstruction and measurement must follow according to the required inspection protocol and the workflow of Fig. 3. Although the measurement inspection is far from the

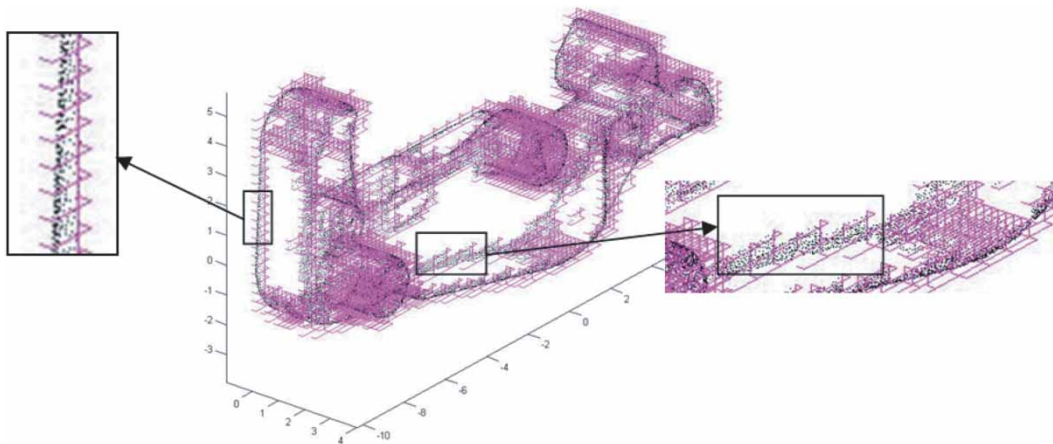
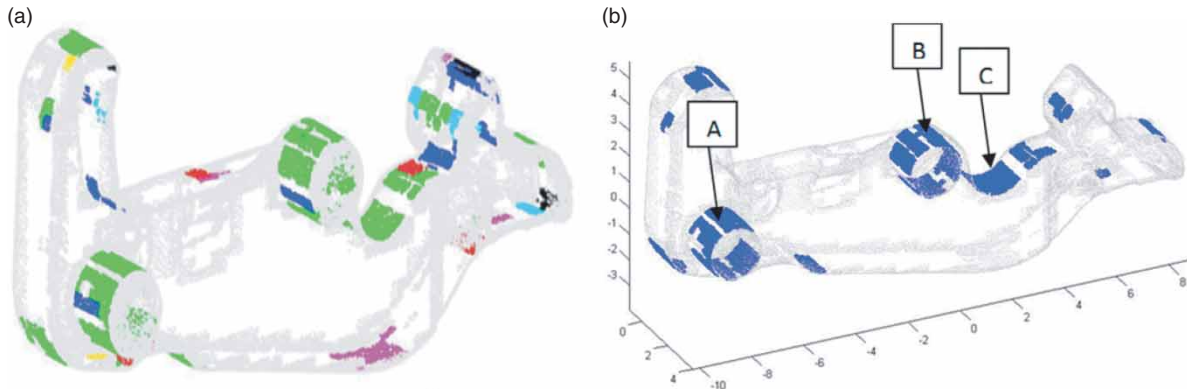


Figure 9. Curved voxels recognized in the lever before cylinder recognition.

Table 1. Automatic selection of variance threshold for finding cylindrical voxels.

Directions	Initial number of bins	Final number of bins (optimal)	Variance Threshold (mm ²)	Initial number of curved voxels	Final number of cylindrical voxels
Direction X	20	55	$3,42 \times 10^{-6}$	793	569
Direction Y	20	48	$6,91 \times 10^{-6}$	262	62
Direction Z	20	48	$5,45 \times 10^{-6}$	333	82
Total				1388	713

**Figure 10.** (a) Set of points of the clusters found in the X-direction; (b) Cluster of R1 cylinders.

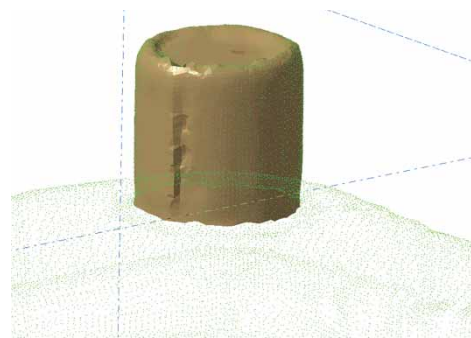
aim of this paper, to give a preliminary evaluation of the soundness of the proposed approach cylinders A, B and C of Fig. 10(b) have been compared with the interactive post-processing made by Catia. In this case Cylinder A has a effective value of $R = 0.974$ mm, $R = 0.972$ mm for Cylinder B and $R = 0.999$ mm for Cylinder C. Standard deviation of the fittings are always less than 0.012 mm. For the proposed algorithm the radii of the single clusters are: 0.974 mm for cylinder A and B, 1.036 mm for cylinder C with a standard deviation less than 0.006 mm.

5. Discussion

Considering the works [4] and [5] the latching lever represents the third test case analysed by the proposed approach. Also in this case the proposed segmentation procedure based on the Hierarchical Space Partitioning is able to distinguish planar local surfaces from curved and from them, cylindrical ones. The voxel structure is opportune to save calculation time, limiting the analysis only on the true-state voxels. In this case, the number of true-state voxels is 3077 compared to the total of 32768 voxels, with a proportion of about 1:10. This allows to reduce the time of computation considering that they include and allow to analyse more than 62×10^3 points. Moreover the iterative adoption of a similar scheme of processing for both planar and curved voxels and the adoption of parallel computing allow to spare time and memory.

Concerning the cylinder analysis via LM(Kasa) circle fit, although some limits have been confirmed in Section 3, it is able to analyse the latching lever and to be integrated in the hybrid region-growing and hierarchical clustering procedure applied to clustering together voxels with similar characteristics.

Obviously the automation through the adoption of thresholds on the L2 norms adopted for the aggregation makes lose accuracy in the final number of voxels included in the final clusters. It is clearly shown in Fig. 11. where the local tessellation of cylinder A of Fig. 10 has been. made manually by Catia. It highlights local discontinuity of the cloud (probably due to an error of the multiple view composition and to a surface embossment caused by shrinkage) that corresponds to local absence of voxels in that part of the cluster.

**Figure 11.** Local tessellation of cylinder A to highlights local discontinuities.

6. Conclusions


The main conclusions of the work are:

- the proposed post-processing addresses the goal of an automatic post-processing for both cylindrical and planar surfaces;
- cylindrical surface partition and clusterization made coupling Kasa and LM algorithms is effective for the number of points typically found in our voxel structure and literature data about approximation error are confirmed;
- the definition of the IRS helps to avoid CAD model alignment, that becomes unnecessary for the measurement;
- concerning the criterion for defining which are planar or cylindrical voxels, the adoption of an iterative analysis of the variance frequency histogram seems to mitigate the previous arbitrary assignment of thresholds, although more accurate sensitivity analysis must be done to evaluate its robustness
- Voxel resolutions represents the intrinsic limit of the procedure but also its strength to classify surfaces digitized with a large number of points. In addition, more accurate investigations about time of computation are required.

Finally the investigation of the sensitivity to the threshold applied to the L2 norm for cylinder clusterization must be done together with the definition and validation of the two last steps of the proposed procedure, Cylinder reconstruction and measurement.

ORCID

Michele Bici  <http://orcid.org/0000-0002-7744-2152>

Francesca Campana  <http://orcid.org/0000-0002-6833-8505>

References

- [1] Al-Sharadqah, A.; Chernov, N.: Error analysis for circle fitting algorithms. *Electron. J. Statist.* 3, 886–911. <http://dx.doi.org/10.1214/09-EJS419>, 2009.
- [2] Attene, M.; Falcidieno, B.; Spagnuolo, M.: Hierarchical mesh segmentation based on fitting primitives, *The Visual Computer*, 22(3), 2006, 181–193. <http://dx.doi.org/10.1007/s00371-006-0375-x>
- [3] Beiter, K. A.; Ishii, K.: Incorporating dimensional requirements into material selection and design of injection molded parts, 1997, Annual Technical Conference - ANTEC, Conference Proceedings, 3, pp. 3295–3299.
- [4] Bici, M; Campana, F; Petriaggi, S.; Tito, L.: Study of a point cloud Segmentation with Part Type Recognition for tolerance inspection of plastic components via Reverse Engineering, *Computer Aided Design and Application*, 11(6), 2014, 640–648. <http://dx.doi.org/10.1080/16864360.2014.914382>
- [5] Bici, M; Campana, F; Trifirò, A.; Testani, C.: Development of automatic tolerance inspection through Reverse Engineering, *Proceeding of Metrology for Aerospace (MetroAeroSpace)*, 2014 IEEE, 29–30, Benevento – Italy <http://dx.doi.org/10.1109/MetroAeroSpace.2014.6865903>
- [6] Busick, D. R.; Beiter, K. A.; Ishii, K.: Design for injection molding: Using process simulation to assess tolerance feasibility, *Computers in Engineering, Proceedings of the International Conference and Exhibit*, (1/-), 1994, 113–120.
- [7] Gao, J.; Gindy, N.; Chen, X.: An automated GD&T inspection system based on non-contact 3D digitization, *International Journal of Production Research*, 44(1), 2006, 117–134. <http://dx.doi.org/10.1080/09638280500219737>.
- [8] Kasa, I: A circle fitting procedure and its error analysis, *IEEE Transactions on Instrumentation and Measurement*, IM-25(1), 8,14. <http://dx.doi.org/10.1109/TIM.1976.6312298>
- [9] Keller, P; Bertram, M.; Hagen, H.: Reverse engineering with subdivision surfaces, 2007, *Computing April*, 79(2-4), 2007, 119–129. <http://dx.doi.org/10.1007/s00607-006-0191-1>
- [10] Martínez, S.; Cuesta, E.; Barreiro, J.; Álvarez, B.: Analysis of laser scanning and strategies for dimensional and geometrical control, *Int J Adv Manuf Technol*, 46, 2010, 621–629. <http://dx.doi.org/10.1007/s00170-009-2106-8>
- [11] Shamir A.: A survey on Mesh Segmentation Techniques, *Computer Graphics Forum*, Volume 27, Issue 6, pages 1539–1556, September 2008. <http://dx.doi.org/10.1111/j.1467-8659.2007.01103.x>
- [12] Taubin, G.: Estimation of planar curves, surfaces, and nonplanar space curves defined by implicit equations with applications to edge and range image segmentation, *IEEE Transactions on Pattern Analysis and Machine Intelligence*, 13(11), 1991, 1115–1138. <http://dx.doi.org/10.1109/34.103273>
- [13] Wang, L.; Bi, Z.M.: Advances in 3D data acquisition and processing for industrial applications, *Robotics and Computer-Integrated Manufacturing*, 26, 2010, 403–413. <http://dx.doi.org/10.1016/j.rcim.2010.03.003>